

# Silicon Nanowire-Based Surface-Enhanced Raman Spectroscopy Endoscope for Intracellular pH Detection

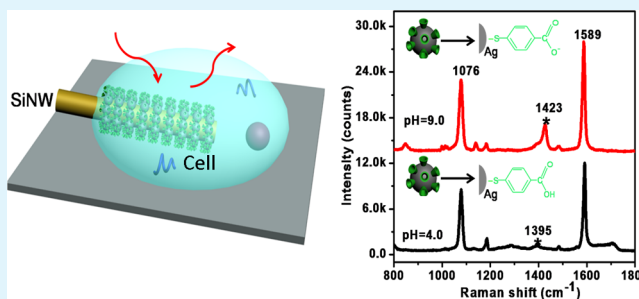
Xuemei Han, Hui Wang,\* Xuemei Ou, and Xiaohong Zhang\*

Nano-organic Photoelectronic Laboratory and Key Laboratory of Photochemical Conversion and Optoelectronic Materials, Technical Institute of Physics and Chemistry, Chinese Academy of Sciences, Beijing, 100190, People's Republic of China

## Supporting Information

**ABSTRACT:** Very recently, one-dimensional nanowire (NW) sensors have attracted great attention as smart optical endoscopes to probe and manipulate intracellular biological processes. However, NWs often have limited optical response to the intracellular environment changes. In this work, a near-infrared nanowire optical endoscope for high-resolution intracellular pH detection was developed by integrating the advantages of silicon nanowires and surface-enhanced Raman spectroscopy (SERS). This optical endoscope has a high-resolution, sensitive response to local pH changes over the wide range of pH 4.0–9.0, an important range for most biological processes in cells, with high reproducibility, good reversibility, and at least one-week stability in an aqueous environment. The results indicate the great potential of a single SiNW SERS endoscope for intracellular pH monitoring.

**KEYWORDS:** silicon nanowire, optical endoscope, surface-enhanced Raman spectroscopy, intracellular pH probing, near-infrared spectrum, high sensitive sensor



## INTRODUCTION

One-dimensional (1D) nanomaterials can feasibly penetrate into living cells with minimum perturbation and enable direct physical access to the cell interiors. This ability has given rise to considerable applications, such as endoscopes to probe and manipulate biological processes in living cells.<sup>1–3</sup> Silicon nanowires (SiNWs) are some of the most favorable nanosensor materials for probing intracellular or intercellular environments because of their good biocompatibility, mechanical flexibility, and stability.<sup>4–8</sup> Moreover, SiNWs have high surface-to-volume ratio and one-dimensional nanoscale morphology that are favorable for quick diffusion of analyte molecules into and out of the nanosensor. Thus, they then can increase the reaction rate and consequently lead to a higher sensitivity with faster response and recovery time. Importantly, SiNWs can be integrated with the integrated circuit and optical fiber by using the conventional lithography technique with low cost and great miniaturization potential. SiNW sensors can be fabricated based on their electric and optical properties, respectively.<sup>9,10</sup> The electric properties based field-effect-transistor (FET) sensor has potential advantages in terms of fabrication with well-established microelectronic techniques, while the optical sensors have the advantage of direct physical access to the small detection space such as the cell's interiors and providing spectroscopic fingerprinting information.<sup>11</sup> Furthermore, vibrational information from the molecule's spectrum could provide insights into a wide range of chemical and biological processes, which is of great interest in the application of SiNW sensors as puncture sensors. However, SiNWs have limited optical

response to changes in the intracellular environment. This requires the use of suitable information-reporter molecules to make SiNWs efficiently respond and transmit data on the changes occurring inside the cells. So far, fluorescence techniques are well established and have been used to detect a wide range of molecules (e.g., DNA and CO<sub>2</sub>) and pH values.<sup>12</sup> Nevertheless, fluorescent molecules are often excited and emit light in the visible region (400–700 nm). Thus, the input and output of optical information is significantly attenuated due to multiple scattering caused by cell walls and the strong absorption of hemoglobin (blood) and water.<sup>13</sup>

Surface-enhanced Raman spectroscopy (SERS), an alternative approach to fluorescence, can efficiently overcome the above-mentioned challenges. The excitation wavelengths can be in the red and near-infrared (NIR) regions of the spectrum, which is known as a “clear window” for optical imaging and sensing in living systems.<sup>14,15</sup> Within this window, the input and output of optical signals can readily pass through cells and tissues, and autofluorescence is also minimized. SERS can provide rich molecular information and be incorporated into fiber-optic systems.<sup>16</sup> To date, a large number of biological applications of SERS in living systems have been reported. For example, Qian et al.<sup>17</sup> utilized SERS-active gold nanoparticles (NPs) for in vivo tumor targeting and detection. Pallaoro et al.<sup>18</sup> developed silver NP (AgNP) clusters as SERS probes for

Received: April 16, 2013

Accepted: May 31, 2013

Published: May 31, 2013

mapping intracellular environments. However, most of these reports are based on randomly aggregated colloidal NPs that often lead to large variations in the measured SERS signals.<sup>19–21</sup> Local changes cannot be monitored precisely with such mobile NPs. Therefore, integrating the advantages of both SiNWs and SERS is expected to lead to the development of a highly efficient optical endoscope for intracellular detection.<sup>22,23</sup>

In this article, we demonstrate a NIR SiNW-based SERS endoscope for intracellular pH detection with high resolution. The endoscope is fabricated by first depositing uniform, densely packed AgNPs on SiNW (AgNPs@SiNW) and subsequently functionalizing them with pH-sensitive *p*-mercaptobenzoic acid (pMBA) molecules.<sup>18–21</sup> This endoscope has a high-resolution, sensitive response to local pH changes over the wide range of pH 4.0–9.0, an important range for most biological processes in cells.<sup>24</sup> The endoscope also exhibits high reproducibility, good reversibility, and at least one-week stability in an aqueous environment. The results indicate that the single AgNPs@SiNW SERS endoscope has great potential for investigating intracellular biological processes.

## EXPERIMENT SECTION

SiNWs were first synthesized via a typical vapor–liquid–solid process using Sn as catalyst.<sup>25</sup> AgNPs with well-controlled sizes were uniformly deposited on the SiNW surface in the presence of a surfactant following a method recently reported by our laboratory.<sup>26</sup> The details of the experiments are shown in the Supporting Information, S1. Figures 1a and 1b display the transmission electron microscopy

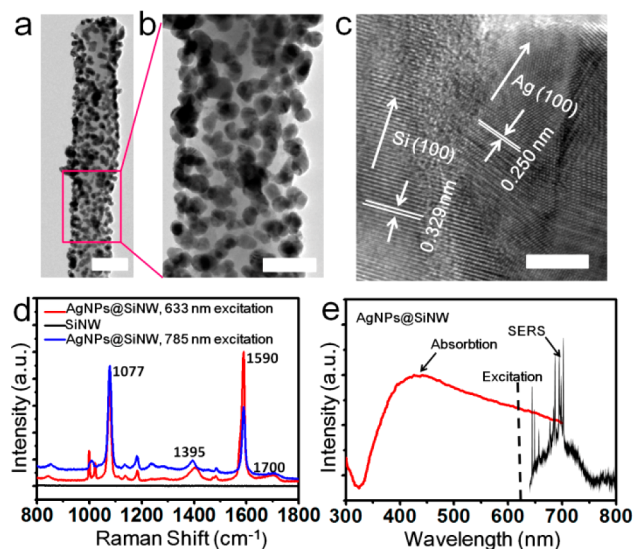


**Figure 1.** (a), (b), and (c) TEM and HR-TEM images of as-prepared AgNPs@SiNW. The scale bars are 200, 100, and 5 nm, respectively. (d) SERS spectra of pMBA adsorbed on a single AgNPs@SiNW and pure SiNW. (e) Optical absorption (red curves) of AgNPs@SiNW and emission spectra of SERS AgNPs@SiNW (black curves).

(TEM) images of the as-prepared sample. Uniform, densely packed AgNPs with diameters ranging from 20 to 30 nm were clearly loaded onto the SiNWs (diameter = 200 nm). The high-resolution TEM image (Figure 1c) shows that the well-defined AgNP structures were immobilized on the SiNW surface. The prepared samples exhibited prominent stability; i.e., the AgNPs did not separate from the SiNWs even after storage or ultrasonication.

To test the Raman enhancement for pMBA, the AgNPs@SiNW was exposed to an aqueous solution of pMBA ( $1 \times 10^{-5}$  M) for one hour to ensure full surface coverage and avoid complications due to nonspecific surface adsorption (Supporting Information, S2). Before the Raman measurements, the sample was thoroughly rinsed with deionized water. As shown in Figure 1d, highly enhanced Raman peaks can be observed from the pMBA adsorbed on AgNPs@SiNW under irradiation with a 633 or 785 nm laser, whereas no visible Raman peak of pMBA can be observed on a pure SiNW. This high enhancing ability mainly arises from the unique morphology of the densely packed AgNPs with well-controlled particle sizes and small interparticle distances (less than 10 nm). The prominent features at 1077 and 1590  $\text{cm}^{-1}$  in the Raman spectra were attributed to the ring breathing modes of pMBA. The other two weak but pH-sensitive Raman bands near 1395 and 1700  $\text{cm}^{-1}$  indicated the presence of dissociated ( $\text{COO}^-$ ) and neutral ( $\text{C}=\text{O}$ ) carboxylic groups, respectively.<sup>18,21</sup> Hence, SiNWs after decoration with AgNPs are highly sensitive, stable, and efficient for SERS endoscope at red and NIR excitations.

## RESULTS AND DISCUSSION

Figure 1e shows the optical absorption of AgNPs@SiNW and the emission spectra (SERS) of the functional molecule-modified AgNPs@SiNW (633 nm excitation). Notably, the NW-based SERS endoscope offered richer spectroscopic information and produced emission peaks that were much narrower than those of fluorescence molecules or quantum dots.<sup>11,17,18</sup>

The high-resolution measurement of localized intracellular pH changes was performed with a single AgNPs@SiNW fixed on the tip of a 10  $\mu\text{m}$  glass pipet. Limited by the difficulty of pH modulation in living cells, the intracellular pH measurement was simulated by penetrating the NW endoscope into a microdroplet (about 1–2  $\mu\text{L}$  in volume) of phosphate-buffered saline with different pH values (Figure 2a). A Ttong F-50 portable pH meter was used to adjust the pH of the buffer to an

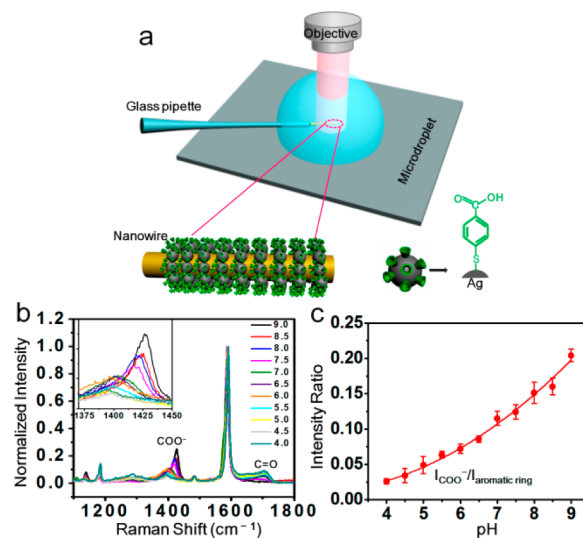


**Figure 2.** (a) Illustration of the stimulative intracellular pH measurement with our SiNW-based endoscope fixed on the tip of a pulled glass pipet. (b) pH-dependent SERS spectra of pMBA functionalized single AgNPs@SiNW. All spectra are normalized by the intensity of 1590  $\text{cm}^{-1}$ . The inset is the peak position shift of  $\text{COO}^-$  mode under pH modulation. (c) pH calibration curve of the signal intensity ratio of the stretching mode of the  $\text{COO}^-$  groups and the ring breaching mode as a function of pH. The fit curve is a guide to the eye.

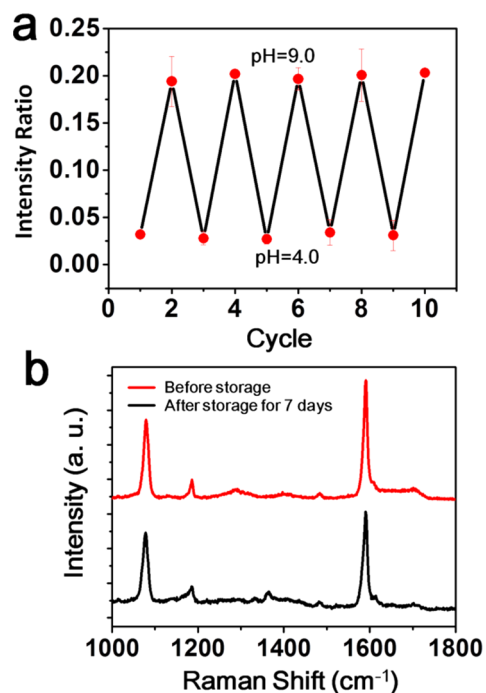
accuracy of 0.01 pH units. The Raman spectra were collected on a single NW with 785 nm excitation. Between measurements, the NW sensor was rinsed thoroughly with deionized water. It should be noted that inserting SiNWs into living cells has been widely studied previously.<sup>1–3</sup> Moreover, the feasibility of this simulation detection method had been proved by Yan et al. in their simulated intracellular pH measurement.<sup>11</sup>

Figure 2b reveals the high-sensitivity SERS spectra of the NW response as a function of pH ranging from 4.0 to 9.0. With increasing pH of the solution, the intensity of the mode of  $\text{COO}^-$  significantly increased. This finding can be attributed to the increased number of dissociated carboxyl groups. Correspondingly, the intensity of the mode of  $\text{C}=\text{O}$  decreased. The peak position of the  $\text{COO}^-$  mode shifted from 1395 to 1423  $\text{cm}^{-1}$  with increasing pH beyond 7.0. This peak position shift may arise from the changes in the interaction between the AgNP surface and  $\text{COO}^-$  groups.<sup>21</sup> In acidic environments, carboxylic groups become nearly neutral and slightly hydrophobic and thus condense on the AgNP surface.<sup>27</sup> The dissociation of carboxylic groups is weak under such conditions but still occurs because of the reduction of the  $\text{pK}_a$  of pMBA when it is covalently attached to a metal surface.<sup>28</sup> Consequently, a few  $\text{COO}^-$  groups are produced and trapped on AgNP surfaces by hydrophobic carboxylic groups, inducing the appearance of a broad band at 1390  $\text{cm}^{-1}$ .<sup>21</sup> However, in alkaline environments, most carboxylic groups appear as free-standing  $\text{COO}^-$  formed on AgNPs due to their hydrophilicity, thus presenting a narrower and higher wavenumber band at 1423  $\text{cm}^{-1}$ .<sup>21</sup>

To clarify the performance of the sensor, the SiNW-based SERS endoscope was used to detect the pH value of the cell-culture medium: Hyclone DMEM (high glucose), with L-glutamine, without sodium pyruvate (contains 10% fetal bovine serum). The pH value (8.34) of the cell-culture medium was first measured by A Ttong F-50 portable pH meter and then by the SiNW sensor. The signal intensity ratio of the stretching mode of the  $\text{COO}^-$  groups and the unchanged aromatic ring breaching mode (1590  $\text{cm}^{-1}$ ) was 0.145. The result is in accordance with the pH of phosphate-buffered saline solution. Therefore, it is proposed that the proteins and cell contaminants may have an ignorable affect on the performance of the SiNW SERS sensor.

The signal intensity ratio of the stretching mode of the  $\text{COO}^-$  groups and the unchanged aromatic ring breaching mode (1590  $\text{cm}^{-1}$ ) can be used as indicators to monitor the environmental pH changes.<sup>18–20</sup> Figure 2c shows the plot of pH against this Raman intensity ratio. The error bars represent the standard deviation of measurements with the same pH value. The average percentage error was about 5.06%, suggesting that a single AgNPs@SiNW was more precise and reliable than colloidal AgNPs and Au nanostructures in local pH-sensing applications.<sup>19,20</sup> These highly reproducible and reliable pH measurements can be attributed to the well-defined and uniform AgNP structure on the SiNW surface. This unique structure can generate abundant SERS-active sites with consistent SERS responses.<sup>26</sup> On the contrary, the random AgNP aggregations with various morphologies that are commonly used in traditional SERS measurements are very likely to introduce large errors and low-efficiency SERS signals due to their largely different hot sites.<sup>19,20</sup>

Apart from highly sensitive pH detection, the SiNW-based endoscope also exhibits excellent repeatability and reversibility. Figure 3a shows the Raman intensity ratios of the  $\text{COO}^-$  group



**Figure 3.** (a) Repeatability and reversible recording of the intensity ratios of  $I_{\text{COO}^-}$  and  $I_{\text{aromatic ring}}$  by alternate measurement in two solutions with pH 4.0 and 9.0. (b) SERS spectra recorded from pMBA functionalized AgNPs@SiNW before and after storage in DI water for 7 days.

and aromatic ring that are alternately measured in two solutions with pH 4.0 and 9.0, respectively. It reveals a negligible signal ratio drift and good photostability under illumination in five cycles. The good repeatability is characterized by the low relative standard deviation (RSD) values of 9.54% (pH 4.0) and 1.85% (pH 9.0). The relatively lower RSD in the alkaline condition may be due to the unique property of pMBA molecules that enables  $\text{COO}^-$  groups to exhibit higher sensitivity in alkaline solutions.<sup>29</sup>

From the viewpoint of practical application, the storage stability of a pH sensor is also an important feature. Figure 3b displays the SERS spectra obtained from freshly prepared pMBA-AgNPs@SiNW and from that stored in deionized water (pH 7.0) for about 7 days. Notably, there was no significant change observed in both the Raman peak position and signal intensity. Thus, the SiNW-based SERS endoscope can stably work for at least one week in the aqueous phase. This considerable stability can be attributed to the stable morphology of SERS-active AgNPs during immersion in an aqueous environment.<sup>26</sup> This long-term stability is important in the handling of the NW-based endoscope for practical applications.

## CONCLUSION

In summary, an optical endoscope comprising AgNP-modified SiNWs was developed for high-resolution, reproducible intracellular pH detection with NIR excitation using the SERS technique. This NW endoscope can provide very rich spectroscopic information and enables the high-resolution, sensitive detection of pH changes close to the NW over a wide range (pH 4.0–9.0). It also exhibits good reproducibility, good reversibility, and long-term stability in an aqueous environment. The results suggest that the SiNW-based SERS endoscope will

provide new opportunities for direct sensing in living cells and studying biological mechanisms with rich molecular fingerprinting information.

## ■ ASSOCIATED CONTENT

### Supporting Information

Sample preparation and characterization and absorption of pMBA molecules on AgNPs@SiNW at different concentrations. This material is available free of charge via the Internet at <http://pubs.acs.org>.

## ■ AUTHOR INFORMATION

### Corresponding Author

\*E-mail: [xhzhang@mail.ipc.ac.cn](mailto:xhzhang@mail.ipc.ac.cn); [wanghui@mail.ipc.ac.cn](mailto:wanghui@mail.ipc.ac.cn).

### Author Contributions

The manuscript was written through contributions of all authors. All authors have given approval to the final version of the manuscript.

### Notes

The authors declare no competing financial interest.

## ■ ACKNOWLEDGMENTS

The work was partially supported by the National Basic Research Program of China (973 Program) (Grant No. 2010CB9345000, 2012CB932400), the Major Research Plan of the National Natural Science Foundation of China (Grant No. 91233110), and Beijing Natural Science Foundation (Grant No. 2112044).

## ■ REFERENCES

- (1) Obataya, I.; Nakamura, C.; Han, S.; Nakamura, N.; Miyake, J. *Nano Lett.* **2005**, *5*, 27–30.
- (2) Singhal, R.; Orynbayeva, Z.; Sundaram, R. V. K.; Niu, J. J.; Bhattacharyya, S.; Vitol, E. A.; Schrlau, M. G.; Papazoglou, E. S.; Friedman, G.; Gogotsi, Y. *Nat. Nanotechnol.* **2011**, *6*, 57–64.
- (3) Lee, Y. E. K.; Kopelman, R. *Nat. Nanotechnol.* **2012**, *7*, 148–149.
- (4) Shalek, A. K.; Robinson, J. T.; Karp, E. S.; Lee, J. S.; Ahn, D. R.; Yoon, M. H.; Sutton, A.; Jorgolli, M.; Gertner, R. S.; Gujral, T. S.; MacBeath, G.; Yang, E. G.; Park, H. *Proc. Natl. Acad. Sci. U.S.A.* **2010**, *107*, 1870–1875.
- (5) He, Y.; Zhong, Y. L.; Peng, F.; Wei, X. P.; Su, Y. Y.; Su, S.; Gu, W.; Liao, L. S.; Lee, S. T. *Angew. Chem., Int. Ed.* **2011**, *50*, 3080–3083.
- (6) Kim, W.; Ng, J. K.; Kunitake, M. E.; Conklin, B. R.; Yang, P. D. *J. Am. Chem. Soc.* **2007**, *129*, 7228–7229.
- (7) Kilian, K. A.; Bocking, T.; Gaus, K.; King-Lacroix, J.; Gal, M.; Gooding, J. J. *Chem. Commun.* **2007**, *19*, 1936–1938.
- (8) Lv, M.; Su, S.; He, Y.; Huang, Q.; Hu, W.; Li, D.; Fan, C.; Lee, S. T. *Adv. Mater.* **2010**, *22*, 5463.
- (9) Kuang, Q.; Lao, C. S.; Wang, Z. L.; Xie, Z. X.; Zheng, L. S. *J. Am. Chem. Soc.* **2007**, *129*, 6070.
- (10) Mu, L. X.; Shi, W. S.; Chang, J. C.; Lee, S. T. *Nano Lett.* **2008**, *8*, 104–109.
- (11) Yan, R. X.; Park, J. H.; Choi, Y.; Heo, C. J.; Yang, S. M.; Lee, L. P.; Yang, P. D. *Nat. Nanotechnol.* **2012**, *7*, 191–196.
- (12) Epstein, J. R.; Walt, D. R. *Chem. Soc. Rev.* **2003**, *32*, 203–214.
- (13) Yuen, J. M.; Shah, N. C.; Walsh, J. T.; Glucksberg, M. R.; Van Duyne, R. P. *Anal. Chem.* **2010**, *82*, 8382–8385.
- (14) Wachsmann-Hogiu, S.; Weeks, T.; Huser, T. *Curr. Opin. Biotechnol.* **2009**, *20*, 63–73.
- (15) Mahmood, U.; Weissleder, R. *Mol. Cancer Ther.* **2003**, *2*, 489–496.
- (16) Pesapane, A.; Lucotti, A.; Zerbi, G. *J. Raman Spectrosc.* **2010**, *41*, 256–267.
- (17) Qian, X. M.; Peng, X. H.; Ansari, D. O.; Yin-Goen, Q.; Chen, G. Z.; Shin, D. M.; Yang, L.; Young, A. N.; Wang, M. D.; Nie, S. M. *Nat. Biotechnol.* **2008**, *26*, 83–90.
- (18) Pallaoro, A.; Braun, G. B.; Reich, N. O.; Moskovits, M. *Small* **2010**, *6*, 618–622.
- (19) Talley, C. E.; Jusinski, L.; Hollars, C. W.; Lane, S. M.; Huser, T. *Anal. Chem.* **2004**, *76*, 7064–7068.
- (20) Schwartzberg, A. M.; Oshiro, T. Y.; Zhang, J. Z.; Huser, T.; Talley, C. E. *Anal. Chem.* **2006**, *78*, 4732–4736.
- (21) Michota, A.; Bukowska, J. *J. Raman Spectrosc.* **2003**, *34*, 21–25.
- (22) He, Y.; Su, S.; Xu, T. T.; Zhong, Y. L.; Zapfen, J. A.; Li, J.; Fan, C. H.; Lee, S. T. *Nano Today* **2011**, *6*, 122–130.
- (23) Wei, X. P.; Su, S.; Guo, Y. Y.; Jiang, X. X.; Zhong, Y. L.; Su, Y. Y.; Fan, C. H.; Lee, S. T.; He, Y. *Small* **2012**, DOI: 10.1002/small.201202914.
- (24) Srivastava, J.; Barber, D. L.; Jacobson, M. P. *Physiology* **2007**, *22*, 30–39.
- (25) Wang, H.; Zhang, X. H.; Meng, X. M.; Zhou, S. M.; Wu, S. K.; Shi, W. S.; Lee, S. *Angew. Chem., Int. Ed.* **2005**, *44*, 6934–6937.
- (26) Han, X. M.; Wang, H.; Ou, X. M.; Zhang, X. H. *J. Mater. Chem.* **2012**, *22*, 14127–14132.
- (27) Qian, X. M.; Li, J.; Nie, S. M. *J. Am. Chem. Soc.* **2009**, *131*, 7540–7541.
- (28) Bishnoi, S. W.; Rozell, C. J.; Levin, C. S.; Gheith, M. K.; Johnson, B. R.; Johnson, D. H.; Halas, N. J. *Nano Lett.* **2006**, *6*, 1687–1692.
- (29) Zong, S. F.; Wang, Z. Y.; Yang, J.; Cui, Y. *Anal. Chem.* **2011**, *83*, 4178–4183.